scientific reports

Check for updates

OPEN

A preliminary bioinformatic screen to identify SRI SMC2 PSIP1 TLE4 and MSX1 as potential diagnostic and prognostic markers of osteoarthritis

Jolanta Kryczka[1], Ewa Brzeziańska-Lasota[1], Michał Pikuła[2,3], Joanna Boncela[4] & Jakub Mateusz Kryczka[4]✉

Osteoarthritis (OA) is the most common degenerative joint disease, leading to severe pain and functional disability for nearly 530 million people worldwide. OA is characterized by progressive loss of cartilage and synovial hyperplasia from the articulating surfaces of any diarthrodial joints, however, the majority of cases account for the hip and knee. Currently, regenerative therapy based on stem cells has emerged as one of the most promising and rapidly evolving strategies in OA. Although progression and potential regeneration can be monitored by magnetic resonance imaging (MRI), we lack proper molecular markers of joint regeneration for diagnostic and in vitro studies. Gene expression profiles of articular cartilage (chondrocytes) and synovium from OA-affected patients' were downloaded from The Gene Expression Omnibus database (GSE179716, GSE206848, GSE239343, GSE48556) and analyzed using various bioinformatic tools and platforms: GEO2R, FunRich, C-Big, The Human Protein Atlas, STRING, Orange data mining, Jasp, Gene Ontology and Reactome. OA-affected synovium and chondrocytes present differences between aurora B and A signaling. However, major biological pathways are similarly enriched with *SRI*, *SMC2*, *PSIP1*, *TLE4*, and *MSX1* genes identified as prominent molecular biomarkers of OA progression and mesenchymal stem cell-based OA regeneration. Additionally, in peripheral blood mononuclear cells (PBMCs) from OA patients *PSIP1* and *TLE4* present (respectively) down and up-regulated mRNA levels. mRNA expression levels of chosen genes can indicate OA progression mainly in the in vitro studies, whereas the mRNA level ratio of *PSIP1:TLE4* from PBMCs derived from OA patients can help monitor OA progression in clinical practice.

Keywords Osteoarthritis, Osteoarthritis markers, Regenerative medicine, Mesenchymal stem cells, *SRI*, *SMC2*, *PSIP1*, *TLE4*, *MSX1*

Abbreviations

ADAMTS-5	A disintegrin and metalloproteinase with thrombospondin motifs protein 5
AD-MSCs	Adipose tissue-derived mesenchymal stem cells
AUC-ROC	The area under the receiver operating characteristic curve
BP	Biological process
BMP	Bone morphogenic protein
CC	Cellular components
CING	Cyprus Institute of Neurology & Genetics
DEGs	Differently expressed genes
DNA	Deoxyribonucleic acid
EMT	Epithelial to mesenchymal transition

[1]Department of Biomedicine and Genetics, Medical University of Lodz, 92-213 Lodz, Poland. [2]Laboratory of Tissue Engineering and Regenerative Medicine, Division of Embryology, Department of Anatomy, Faculty of Medicine, Medical University of Gdansk, 80-211 Gdańsk, Poland. [3]Department of Biochemistry, University of Physical Education and Sport, 80-336 Gdańsk, Poland. [4]Laboratory of Cellular Signaling, Institute of Medical Biology, Polish Academy of Sciences, 93-232 Lodz, Poland. ✉email: jkryczka@cbm.pan.pl

FGF	Fibroblast growth factor
GEO	The Gene Expression Omnibus database
GO	The Gene Ontology
HPA	The Human Protein Atlas
HPCF	The High-Performance Computing Facility
IGF1	Insulin-like growth factor
IL-1β	Interleukin 1 beta
IL-6	Interleukin 6
MMPs	Matrix metalloproteinases
MRI	Magnetic resonance imaging
mRNA	Messenger ribonucleic acid
MSC	Mesenchymal stem cells
NF-κB	Nuclear factor-kappa B
NSAIDs	Non-steroidal anti-inflammatory drugs
OA	Osteoarthritis
PBMCs	Peripheral blood mononuclear cells
PDGF	Platelet-derived growth factor
PPI	Protein-protein interaction
S1P1	Sphingosine-1-phosphate receptor 1
TGFβ	Transforming growth factor beta
TNF-α	Tumor necrosis factor alpha
USG	Ultrasonography
VEGF	Vascular endothelial growth factor
Wnt	The Wingless and Int-1

Osteoarthritis (OA) - a complex progressive degenerative disease of the whole joint- is one of the most common types of arthritis and the leading form of disability, affecting nearly 530 million patients worldwide (approximately 7% of the total human population)[1]. Globally, in the past 30 years, the incidence rate of OA increased by 113.25%, from 247.51 million OA-affected patients in 1990 to 527.81 million in 2019[2]. Clinical data showed that OA is characterized by cartilage degeneration, synovial inflammation, subchondral bone thickening, and osteophyte formation, leading to severe structural alterations of the whole joint, causing pain and decreased joint flexibility[3]. Its etiology and major risk factors can be categorized into two subgroups according to the type of stimuli: (1) mechanical, such as joint injury and obesity that significantly increases wear and tear, and (2) non-mechanical, such as excessive and prolonged inflammation resulting in the generation of reactive oxygen species and chemokine secretion, dysregulation of signaling pathways, and mutations in key genes involved in the development of OA[3–5]. On the molecular basis, OA is characterized by dysregulation of Wnt/β-catenin, NF-κB, TGFβ/BMP and FGF signaling pathways, resulting in increased expression of proteolytic enzymes and pro-inflammatory factors: ADAMTS-5, matrix metalloproteinases (MMP1, MMP2, MMP3, MMP9, MMP13), tumor necrosis factor-alpha (TNF-α), interleukin 1 beta (IL-1β), interleukin 6 (IL-6), as well as the deposition of collagen X, that results in imbalance in the delicate equilibrium of ECM synthesis and degradation in cartilage and synovium as well as altering the subchondral bone quality[4,6,7].

Due to its physiology, cartilage has little self-renewal ability[8]. Currently, no drugs can reverse the progression of OA and prevent long-term disability[9]. The recommended treatments, such as non-steroidal anti-inflammatory drugs (NSAIDs), glucocorticoids, opioids, chondroprotective agents, and cytokine inhibitors, reduce the pain and improve joint functionality[10,11]. Recently, regenerative therapy based on mesenchymal stem cells (MSC) has emerged as one of the most promising and rapidly evolving strategies to treat OA[12]. In the case of OA patients, the course of the disease can be monitored by magnetic resonance imaging (MRI) and ultrasonography (USG)[13]. However, standard MRI analyses can predominantly detect alterations seen in the advanced stages of OA and might possess low sensitivity for early, subtle, and potentially reversible changes[14]. OA affecting the whole joint, dysregulates molecular, structural, and physiological homeostasis of different cell/tissue types, that create joints and significantly change their biochemical properties. Therefore, the identification of precise molecular markers that could be utilized to monitor OA progression and potential incremental regeneration and therapeutic outcomes is an urgent matter.

Recently, bioinformatic analyses of genomic, transcriptomic, and proteomic data, often supported by AI-driven engines, by simultaneous analysis of hundreds of records, proved to be useful in the selection of the new markers or important, dysregulated signaling pathways in many different disorders such as cancer or acute myocardial infarction[15–18]. Herein, we present the application of integrated bioinformatic tools to analyze transcriptomic data of OA-affected patients deposited in the publicly available Gene Expression Omnibus database (GEO) to identify genes encoding proteins directly involved in osteoarthritis development that could be utilized as prognostic biomarkers.

Materials and methods

Microarray data processing and analysis

Gene expression profiles with accession numbers: GSE were downloaded from the Gene Expression Omnibus (GEO) database (http://www.ncbi.nlm.nih.gov/geo/ accessed on 30 December 2024) and analyzed similarly to our previous work using the GEO2R online tool and integrated bioinformatics[16,17]. The Benjamini and Hochberg adjusted p-value (Padj.) from the stats package in R, which is the transformation of the p-value using the false discovery rate (FDR) – [P_values, method="fdr"], was used to set statistically significant differently expressed genes (DEGs)[19].

The GSE179716 dataset is composed of transcriptomic data from chondrocytes derived from OA-affected patients ($n=3$ early stage and $n=3$ late stage). Acquired by Biomedical Informatics, University of Pittsburgh, Pittsburg, PA, USA.

The GSE206848 dataset is composed of transcriptomic data from synovium isolated from $n=7$ normal (non-OA-affected) and $n=9$ late OA patients. Acquired by NYU GROSSMAN SCHOOL OF MEDICINE, New York, NY, USA.

The GSE239343 dataset is composed of transcriptomic data (from $n=3$ independent experiments) from chondrocytes (HC #P10970 https://innoprot.com/), inflamed chondrocytes (TNF-inflamed chondrocytes: cultured in a mix of serum-free DMEM and 1% penicillin/streptomycin with 25 ng/mL TNF), and inflamed chondrocytes treated with conditioned medium and conditioned medium (50 µg/mL) from adipose tissue-derived mesenchymal stem cells (AD-MSCs). Acquired by CIC bioGUNE, Genome Analysis Platform, Bizkaia, Spain as described in[20].

The GSE48556 dataset is composed of transcriptomic data obtained from peripheral blood mononuclear cells (PBMCs) of $n=33$ healthy controls and $n=106$ OA patients, Acquired by Leiden University Medical Center, Department of Molecular Epidemiology, Leiden, Netherlands[21].

Bioethical committee approval and patient consent statements are presented with the original publications[20,21] and datasets, available in The Gene Expression Omnibus at http://www.ncbi.nlm.nih.gov/geo/ reference numbers: GSE239343, GSE179716, GSE206848, and GSE48556.

Enrichment analysis

Functional enrichment software tool FunRich (v3.1.3) (http://www.funrich.org/) supported by Gene Ontology (GO) (http://geneontology.org/) (accessed on 30 December 2024) database was used to compare, analyze, and visualize the Biological Process (BP) and Cellular Components (CC) differences associated with the proteins encoded by differently expressed genes (DEGs) in OA-affected and normal patient samples. The cut of was set using p-value < 0.05.

Hierarchical clustering analysis

After extracting the expression values from the gene expression profiles, a bidirectional hierarchical clustering heatmap of differently expressed genes (DEGs) was calculated and visualized using the Orange open-source machine learning and data visualization platform as previously described by us[16,17].

Pearson correlation analysis

Pearson correlation analysis of chosen DEGs was calculated and visualized using JASP 0.14.1.0 software (https://jasp-stats.org/ accessed on 30 December 2024) with a color depiction of "r" value and significance * $p<0.05$, ** $p<0.005$, and *** $p<0.001$ as previously described by us[16,17].

Radial data visualization

Radial data visualization was performed using Orange data mining 3.31.1 software as described by us using a modified Radial Visualization (RadViz) algorithm[17,22,23]. Briefly: data were subjected to a data-driven linear transformation, using the RadViz algorithm, which focuses on visualizing multivariate data in a two-dimensional (2D) space, optimally preserving the data structure. This method visualizes data represented by points inside a circle, using data attributes (mRNA expression level) of N number variables (genes) equidistantly distributed along the circle's circumference. Next, data are placed as points in a location set by the mutual interaction of attributes of N variables, assuming that the greater the attribute value, the closer the data point is drawn. Thus, finally, the data point is placed where the sum of all forces generated by the data value equals 0[22,23]. The homogeneity of formed data clusters was verified using Inner Cluster Deviation (wc).

$$wc = \sum_{i}^{n} \sum_{x \in Ci} d(x,\ ri\ )$$

ri center of *Ci* cluster.

Protein-protein interaction (PPI) network

A PPI network of proteins encoded by chosen genes was created using STRING version 12.0 online software (https://string-db.org/). Network analysis was performed using Cytoscape software version 3.9.1 (https://cytoscape.org/), the Gene Ontology (GO) database (https://amigo.geneontology.org/) and the Reactome database (https://reactome.org/) as previously reported in[16,24]. Active interaction source: "Text-mining", "Experiments", "Databases", "Co-expression", "Neighborhood", "Gene Fusion", "Co-occurrence". Minimum required interaction score: 0.4. Data were additionally verified using the Reactome 2015 database and the Pathway-to-Gene option of the Pathway Connector bioinformatics web tool (https://bioinformatics.cing.ac.cy/) run by the Bioinformatics Department (C-BIG) at the Cyprus Institute of Neurology & Genetics (CING) and the High-Performance Computing Facility (HPCF) of the Cyprus Institute (CyI).

Protein visualization

The tissue sections (immunohistochemistry) and immunofluorescence (confocal microscopy) images of cellular localization of proteins encoded by chosen genes were downloaded from The Human Protein Atlas (HPA) (https://www.proteinatlas.org/)[25]. Immunohistochemistry imaging was performed using antibodies: anti-Sorcin (HPA073666), anti-Structural Maintenance Of Chromosomes 2 (HPA071309), anti-PC4 And SRSF1 Interacting Protein 1 (HPA019697), and anti-Msh Homeobox 1 (CAB026198). Transducin-like enhancer of split

protein 4 tissue immunohistochemistry data are not available (NA) in the HPA database. Immunofluorescence imaging was performed using U-2 OS human osteosarcoma cell line and antibodies: anti-Sorcin (HPA019004), anti-Structural Maintenance Of Chromosomes 2 (HPA071309), anti-PC4 And SRSF1 Interacting Protein 1 (HPA019697), anti-Transducin-like enhancer of split protein 4 (HPA065357), and anti-Msh Homeobox 1 (HPA063895).

Construction of the receiver operating characteristic curve (ROC)

To evaluate the predictive capabilities of the chosen gene, the Area Under the Receiver Operating Characteristic curve (AUC-ROC) curve was calculated and visualized using the JASP 0.16.0.0 software.

Statistics

Statistical evaluation was performed using the normality test (Shapiro–Wilk) followed by the T-Student test (for normally distributed data) or Mann-Whitney U test (for not normally distributed data). Multifactorial statistical evaluation was performed using the ANOVA (one-way) test with Tukey post hoc correction. Calculations and graphs were performed using Orange data mining 3.31.1 software and JASP 0.16.0.0 software; p values < 0.05 were considered statistically significant for all analyses: * $p < 0.05$; ** $p < 0.005$; *** $p < 0.001$, NS-not statistically significant.

Results.

Identification of major OA-related dysregulated genes and biological processes enrichment

OA, as a complex joint degenerative condition, affects several tissue and cell types, resulting in different molecular responses. Thus, to select useful molecular markers to monitor OA progression and joint regeneration upon given therapy, we decided to analyze chondrocytes and synoviocytes from normal and OA-affected knees to find dysregulated genes and molecular pathways (workflow schematic depiction is presented in Fig. 1). We downloaded patients' transcriptomic data deposited in the Gene Expression Omnibus database: the GSE179716 data set is composed of transcriptomic data from chondrocytes derived from OA-affected patients, and the GSE206848 data set is composed of transcriptomic data from synovium. Next, using the GEO2R tool, statistically significant (Padj.<0.05), differently expressed genes (DEGs) were selected for further analysis, receiving 1683 up regulated and 1641 down regulated genes for OA-affected synoviocytes and respectively 3038 and 1513 for OA-affected chondrocytes. Using the Gene Ontology database, and functional enrichment analysis platform FunRich, we noticed that many biological pathways were similarly affected by ongoing OA in both chondrocytes and synovium (Tables 1 and 2). However, significant differences were also noticed, especially once including Aurora B and A signaling that may cause senescence and heterochromatin instability, EMT, and overall

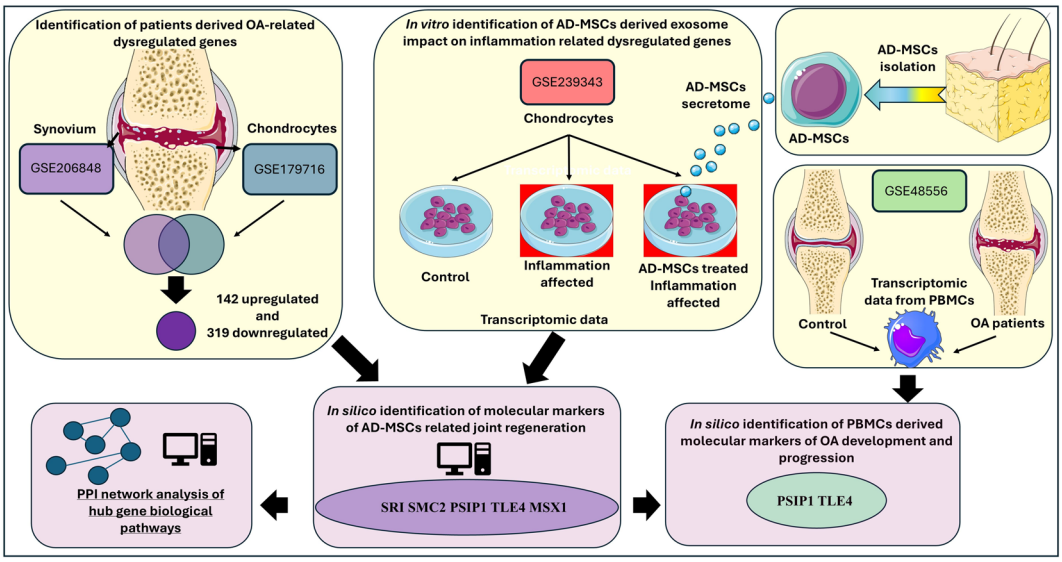

Fig. 1. Schematic presentation of research design. GSE179716 and GSE206848 datasets were analyzed to identify OA-related DEGs (142 upregulated and 319 downregulated) common for chondrocytes and synovium, supported by enrichment analysis. Next, DEGs from control chondrocytes and OA chondrocytes (obtained by TNF-related inflammation) from the GSE239343 dataset were compared to the obtained OA-related DEGs. Common DEGs patterns were then analyzed, and only genes that present dysregulated expression upon OA and regenerated level upon AD-MSC conditioned medium treatment were selected: *SRI*, *SMC2*, *PSIP1*, *TLE4*, and *MSX1*. Biological pathways enrichment of proteins encoded by chosen genes was analyzed using various bioinformatical tools and platforms. Finally, selected genes expression levels were validated in PBMCs using the GSE48556 dataset with *PSIP1* and *TLE4*, presenting significant OA-predictive value. Image provided by Servier Medical Art (https://smart.servier.com/), licensed under CC BY 4.0 (https://creativecommons.org/licenses/by/4.0/).

Biological pathway enriched by up-regulated genes	Percentage of genes involved in enriched pathway		
	OA-affected chondrocytes	OA-affected synoviocytes	*p*
Adherens junctions interactions	0.29%	0.83%	*
Alpha9 beta1 integrin signaling events	27.18%	25.21%	*
Arf6 downstream pathway	26.60%	25.21%	*
Arf6 signaling events	26.60%	25.21%	*
Arf6 trafficking events	26.60%	25.21%	*
Aurora A signaling	2.03%	0.62%	*
Aurora B signaling	2.03%	0.62%	*
Axon guidance	6.69%	4.75%	*
Beta1 integrin cell surface interactions	30.38%	25.41%	***
Beta3 integrin cell surface interactions	2.33%	0.41%	**
Cell cycle. mitotic	9.16%	4.96%	**
Cell-extracellular matrix interactions	1.16%	0.21%	*
Class I PI3K signaling events	26.60%	25.21%	*
Class I PI3K signaling events mediated by Akt	26.60%	25.21%	*
C-MYC pathway	4.22%	2.69%	*
Cyclin D associated events in G1	1.16%	0.41%	*
DNA replication	7.12%	4.34%	*
EGF receptor (ErbB1) signaling pathway	26.60%	25.21%	*
EGFR1	2.76%	3.31%	*
EGFR-dependent endothelin signaling events	26.74%	25.21%	*
Endothelins	27.47%	25.62%	**
Epithelial-to-mesenchymal transition	5.96%	1.03%	**
ErbB receptor signaling network	26.89%	25.41%	*
ErbB1 downstream signaling	26.60%	25.21%	*
FOXM1 transcription factor network	2.18%	0.62%	*
Gene expression	0.87%	3.72%	*
Glucocorticoid receptor regulatory network	1.16%	2.07%	*
Glypican 1 network	26.89%	25.21%	*
Glypican pathway	28.05%	25.83%	**
GMCSF-mediated signaling events	26.60%	25.21%	*
Hormone-sensitive lipase (HSL)-mediated triacylglycerol hydrolysis	0.29%	1.45%	*
IFN-gamma pathway	26.6%	25.21%	*
IGF1 pathway	26.74%	25.21%	*
IL1-mediated signaling events	5.38%	4.34%	*
IL3-mediated signaling events	26.6%	25.21%	*
IL5-mediated signaling events	26.60%	25.21%	*
Insulin pathway	26.60%	25.21%	*
Integrin cell surface interactions	3.63%	1.45%	***
Integrin family cell surface interactions	30.81%	25.41%	***
Internalization of ErbB1	26.60%	25.21%	*
LKB1 signaling events	27.33%	25.41%	*
Metabolism of RNA	1.74%	3.31%	*
Mitotic M-M/G1 phases	6.54%	4.34%	*
mTOR signaling pathway	26.60%	25.21%	*
Muscle contraction	2.76%	1.65%	***
Olfactory signaling pathway	0.15%	1.86%	*
PAR1-mediated thrombin signaling events	27.18%	25.21%	*
PD-1 signaling	0.00%	0.41%	*
PDGF receptor signaling network	26.74%	25.21%	*
PDGFR-beta signaling pathway	26.60%	25.21%	*
Plasma membrane estrogen receptor signaling	27.33%	25.21%	**
Proteoglycan syndecan-mediated signaling events	28.49%	25.83%	**
Response to elevated platelet cytosolic Ca2+	2.33%	0.83%	**
S1P1 pathway	26.60%	25.21%	*
Signaling events mediated by focal adhesion kinase	26.60%	25.21%	*
Continued			

Biological pathway enriched by up-regulated genes	Percentage of genes involved in enriched pathway		
	OA-affected chondrocytes	OA-affected synoviocytes	*p*
Signaling events mediated by hepatocyte growth factor receptor (c-Met)	26.60%	25.21%	*
Signaling events mediated by VEGFR1 and VEGFR2	26.74%	25.21%	*
Smooth muscle contraction	2.47%	0.83%	***
Syndecan-1-mediated signaling events	26.89%	25.21%	*
Syndecan-2-mediated signaling events	3.49%	1.86%	**
Thrombin/protease-activated receptor (PAR) pathway	27.18%	25.21%	*
TRAIL signaling pathway	27.18%	26.03%	*
Urokinase-type plasminogen activator (uPA) and uPAR-mediated signaling	26.60%	25.21%	*
VEGF and VEGFR signaling network	27.03%	25.21%	*

Table 1. Biological pathways enriched by up-regulated genes in OA-affected tissue from the GSE179716 and the GSE206848 data sets. Analysis performed using platform FunRich. * $p < 0.05$; ** $p < 0.005$; *** $p < 0.001$.

mechanisms of gene regulation (Tables 1 and 2). Representative Biological Pathways were presented in Fig. 2A, B. Nevertheless, to find potential molecular biomarkers of OA progression, we have selected genes that were up or downregulated in both OA-affected chondrocytes and synoviocytes, receiving respectively 142 and 319 DEGs (Fig. 3A). Obtained PPI network was further analyzed using Cytoscape 3.9.1. Average metrics, for PPI network of up-regulated genes and for PPI network of down-regulated genes, of how often a node appears on the shortest paths between other nodes – BetweennessCentrality are respectively: 0.036 and 0.019, average shortest path from a node to all other nodes – ClosenessCentrality are: 0.389 and 0.267, numerical depiction of how interconnected a node's neighbors are – ClusteringCoefficient are: 0.234 and 0.265 and the average number of direct interactions (edges) a node has (Degree) 3.037 and 4.172. The highest Degree in the PPI network of up-regulated genes presents AKT1 (22) and for PPI network of down-regulated genes EGFR (44). Analysis of Fold change enrichment of Biological Processes and cellular components proved that the major impact is related to apoptosis, immune response, cell adhesion, migration, cell-matrix degradation, and ion transport (Fig. 3B).

Selection of potential markers for OA regeneration based on AD-MSCs therapy

In the next step of our analysis, we decided to use patient-derived data as reference data to select genes that, in the case of chondrocytes, were dysregulated upon inflammation and restored following the treatment with adipose tissue-derived mesenchymal stem cells (AD-MSCs). Thus, having established common OA-related differently expressed genes (DEGs) for chondrocytes and synoviocytes, we tried to select genes which the expression level would be restored by mesenchymal stem cell-based therapy. Hence, we downloaded data from the GSE239343 data set, composed of transcriptomic data from chondrocytes (named Control), TNF-α treated chondrocytes (named Inflammation), that to some extent mimics OA-related joint inflammation and TNF-α inflamed chondrocytes treated with conditioned medium from adipose tissue-derived mesenchymal stem cells (named MSC CM) as described in method section and in[20]. The selection of potential OA markers was performed in several stages. In the first stage, genes that present significantly different (up or down-regulated) expression levels in TNF-α treated chondrocytes vs. control chondrocytes were identified. Next, the obtained set of genes was verified using our previously established OA-related 142 upregulated and 319 down-regulated genes for both chondrocytes and synoviocytes (Fig. 1). Finally, genes, which expression levels were not affected by MSCs secretome (no significant changes between Inflammation vs. MSC CM groups) were excluded. This approach resulted in the selection of 5 genes: *SRI*, *SMC2*, *PSIP1*, *TLE4*, and *MSX1* (Table 3). Well established molecular markers of OA such as *IL-1B*, *IL6*, *MMP1*, *MMP2*, *MMP3*, *MMP9*, *MMP13* and *ADAMTS5* were additionally tested. As expected, all tested markers presented upregulated mRNA level in TNF-α treated chondrocytes, proving that this in vitro model molecularly resembles OA (data not shown). Interestingly, only *MMP9* level was partially downregulated upon adipose tissue-derived mesenchymal stem cells medium treatment.

SRI, *SMC2*, *PSIP1*, *TLE4*, and *MSX1* mRNA expression levels were analyzed in all chondrocyte variants of the GSE239343 data set, and differences were analyzed using the ANOVA test with Tukey post hoc correction (Fig. 4A). Treatment of inflammation-based damaged chondrocytes with conditioned medium from adipose tissue-derived mesenchymal stem cells leads to full (*SRI*, *SMC2*, *PSIP1*) or partial (*TLE4*, *MSX1*) restoration of normal mRNA expression level observed in control, untreated chondrocytes. Next, to analyze the mutual interaction of chosen genes and verify whether changes in their expression levels correlate to one another during OA progression and regeneration processes, the Pearson correlation matrix was created using combined data of the GSE239343 data set and Orange data mining software as previously described by us (Fig. 4B). Our analysis proves that mRNA expression of *MSX1*, *TLE4*, *PSIP1*, and *SMC2* present very strong, statistically significant mutual correlation efficiency ($r > \pm 0.8$). However, mRNA expression of *SRI*, shows a moderate correlation efficiency ($r > \pm 0.4$) with other analyzed genes, but this correlation is statistically insignificant. Hierarchical clustering analysis allows for the construction of a bidirectional tree diagram (dendrogram), where the most similar subjects are placed on branches that are close together visualizing their mutual relations. Thus, using this technique, we have verified if chosen up and down-regulated genes are located on separate arms of the hierarchical dendrogram (Fig. 4C). This technique additionally visualized mRNA expression as shades of an "inferno" color scheme (Orange data mining). Our analysis proved the possible discriminative ability of chosen genes which was further verified using radial data visualization via the RadViz algorithm and Orange

Biological pathway enriched by down-regulated genes	Percentage of genes involved in enriched pathway		
	OA-affected chondrocytes	OA-affected synoviocytes	*p*
Alpha9 beta1 integrin signaling events	27.79%	24.97%	*
Androgen-mediated signaling	2.19%	4.14%	*
Apoptosis	1.46%	3.38%	*
Arf6 downstream pathway	27.79%	24.65%	*
Arf6 signaling events	27.79%	24.65%	*
Arf6 trafficking events	27.79%	24.65%	*
Autodegradation of the E3 ubiquitin ligase COP1	0.55%	1.53%	*
Beta1 integrin cell surface interactions	29.43%	25.74%	**
Canonical NF-kappaB pathway	0.37%	1.53%	*
Centrosome maturation	0.00%	2.07%	*
Class I PI3K signaling events	27.79%	24.65%	*
Class I PI3K signaling events mediated by Akt	27.79%	24.65%	*
Complement cascade	1.65%	0.11%	*
Cytokine signaling in Immune system	7.68%	3.71%	***
Degradation of beta-catenin by the destruction complex	0.55%	1.74%	*
EGF receptor (ErbB1) signaling pathway	27.79%	24.65%	*
EGFR-dependent endothelin signaling events	27.79%	24.65%	*
Endothelins	28.52%	24.75%	**
Epithelial-to-mesenchymal transition	9.69%	3.71%	***
ErbB receptor signaling network	27.97%	25.08%	*
ErbB1 downstream signaling	27.79%	24.65%	*
Formation and maturation of mRNA Transcript	1.28%	7.09%	***
Gene expression	2.74%	10.58%	***
Glypican 1 network	28.15%	24.75%	*
Glypican pathway	28.70%	25.3%	*
GMCSF-mediated signaling events	27.79%	24.65%	*
HIV infection	1.65%	5.78%	*
HIV life cycle	0.73%	3.93%	***
HIV-1 transcription elongation	0.00%	1.31%	*
IFN-gamma pathway	27.79%	24.86%	*
IGF1 pathway	27.79%	24.65%	*
IL2-mediated signaling events	3.29%	3.71%	*
IL3-mediated signaling events	27.79%	24.65%	*
IL5-mediated signaling events	27.97%	24.65%	*
IL6-mediated signaling events	2.74%	1.53%	**
Initial triggering of complement	1.46%	0.11%	*
Insulin pathway	27.79%	24.65%	*
Integrin family cell surface interactions	30.53%	26.06%	***
Internalization of ErbB1	27.79%	24.65%	*
Late phase of HIV life cycle	0.37%	3.49%	**
LKB1 signaling events	27.97%	24.97%	*
Mitotic M-M/G1 phases	1.28%	5.67%	*
mRNA processing	1.28%	5.56%	***
mRNA splicing	0.55%	3.82%	**
mRNA splicing - major pathway	0.55%	3.82%	**
mTOR signaling pathway	27.79%	24.65%	*
Nectin adhesion pathway	27.97%	24.65%	*
PAR1-mediated thrombin signaling events	28.34%	24.86%	**
PDGF receptor signaling network	27.79%	24.75%	*
PDGFR-beta signaling pathway	27.79%	24.65%	*
Plasma membrane estrogen receptor signaling	27.97%	24.97%	*
Processing of capped intron-containing Pre-mRNA	1.28%	5.02%	***
Proteoglycan syndecan-mediated signaling events	29.07%	25.63%	**
RNA polymerase II transcription	0.37%	3.93%	***
S1P1 pathway	27.79%	24.65%	*
Continued			

Biological pathway enriched by down-regulated genes	Percentage of genes involved in enriched pathway		
	OA-affected chondrocytes	OA-affected synoviocytes	*p*
Signaling by GPCR	6.03%	3.71%	*
Signaling events mediated by focal adhesion kinase	27.79%	24.65%	*
Signaling events mediated by hepatocyte growth factor receptor (c-Met)	27.79%	24.65%	*
Signaling events mediated by VEGFR1 and VEGFR2	27.79%	24.75%	*
Sphingosine 1-phosphate (S1P) pathway	27.97%	25.19%	*
Syndecan-1-mediated signaling events	28.15%	24.75%	*
TGFBR	4.02%	4.25%	**
Thrombin/protease-activated receptor (PAR) pathway	28.34%	24.86%	**
TNF receptor signaling pathway	4.57%	7.31%	*
TRAIL signaling pathway	28.52%	26.06%	*
Transcription	0.73%	5.67%	***
Transcription of the HIV genome	0.00%	2.40%	*
Transport of mature mRNA derived from an intron-containing transcript	0.91%	2.18%	*
Transport of mature transcript to cytoplasm	0.91%	2.29%	*
Urokinase-type plasminogen activator (uPA) and uPAR-mediated signaling	27.79%	24.65%	*
VEGF and VEGFR signaling network	27.97%	24.97%	*

Table 2. Biological pathways enriched by down-regulated genes in OA-affected tissue from the GSE179716 and the GSE206848 data sets. Analysis performed using platform FunRich. * $p < 0.05$; ** $p < 0.005$; *** $p < 0.001$.

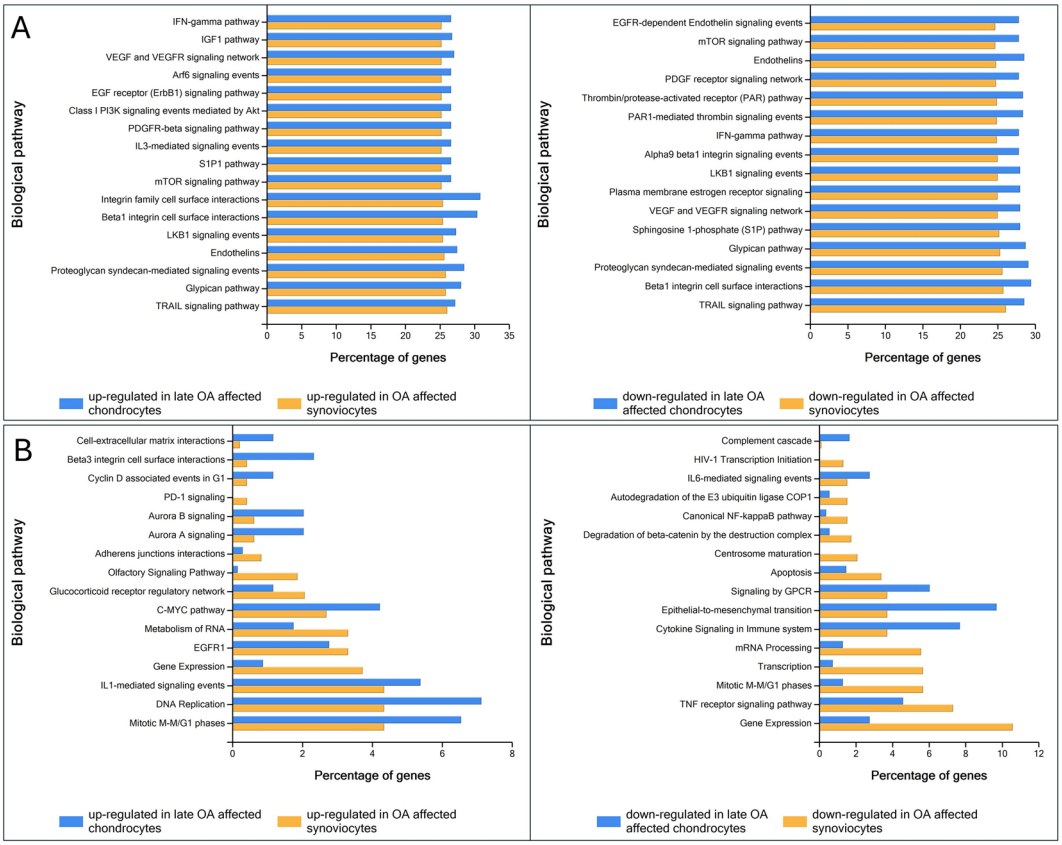

Fig. 2. Functional enrichment analysis of up and down-regulated genes for OA-affected chondrocytes and synoviocytes. Data were downloaded from the GEO database GSE179716 and GSE206848. Major similarly (**A**) and differently (**B**) enriched biological pathways were analyzed using FunRich (v3.1.3) (http://www.funrich.org/) software supported by Gene Ontology (GO) (http://geneontology.org/).

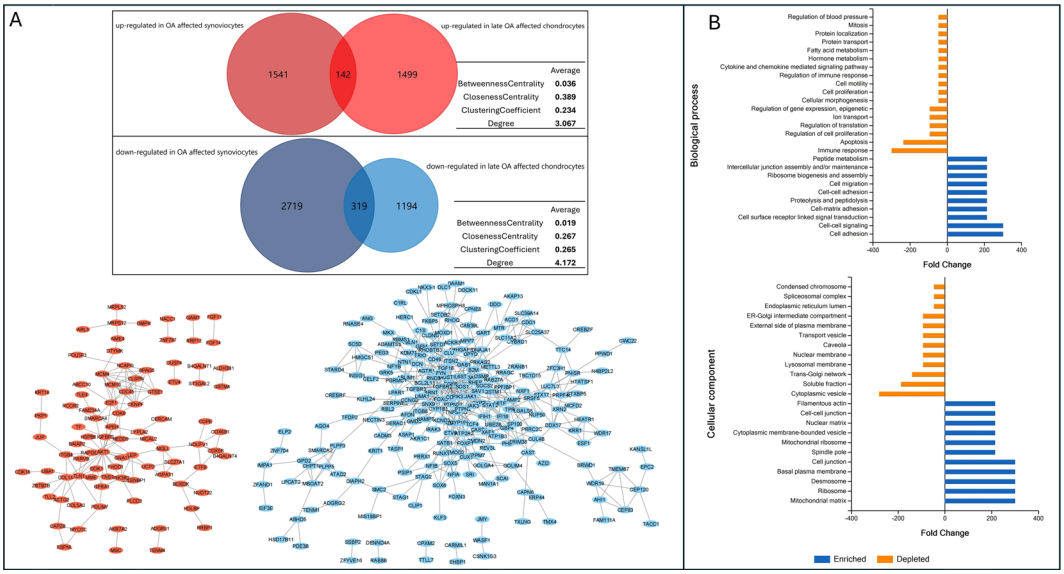

Fig. 3. Selection and functional analysis of OA-related genes. Data were downloaded from the GEO database GSE179716 and GSE206848. 142 upregulated and 319 down-regulated genes commonly dysregulated in OA-affected chondrocytes (GSE179716) and synoviocytes (GSE206848) were selected and visualized by Venn diagram using FunRich (v3.1.3) (http://www.funrich.org/) software (**A**). Protein-protein interaction network visualized using STRING platform. Active interaction source: "Text-mining", "Experiments", "Databases", "Co-expression", "Neighborhood", "Gene Fusion", "Co-occurrence". Minimum required interaction score: 0.4. Network analysis performed via Cytoscape 3.9.1. presenting average value of BetweennessCentrality, ClosenessCentrality, ClusteringCoefficient, and Degree calculated for each obtained network. Analysis of Fold change enrichment of Biological Processes and cellular components performed and visualized using FunRich (v3.1.3) (http://www.funrich.org/) software supported by Gene Ontology (GO) (http://geneontology.org/) (**B**).

Gene	Protein	Note	mRNA level in OA vs. Control
MSX1	Msh Homeobox 1	Muscle segment homeobox gene 1	Upregulated
TLE4	Transducin-like enhancer of split protein 4	Transcriptional corepressor, structural analog to the Drosophila protein Groucho	Upregulated
PSIP1	PC4 And SRSF1 interacting protein 1	Lens epithelium-derived growth factor (LEDGF/p75)	Downregulated
SMC2	Structural maintenance of chromosomes 2	Structural Maintenance Of Chromosomes (SMC) Family Member, Chromosome-Associated Protein E	Downregulated
SRI	Sorcin	Soluble resistance-related calcium-binding protein	Downregulated

Table 3. Selected genes presenting dysregulated mRNA level in OA-affected joint tissues - potential markers of osteoarthritis.

data mining software (3.31.1) (Fig. 4D). This method was recently described by us in[17], briefly: the greater the attribute value, the closer the data point is drawn, and as a result, the data point is placed where the sum of all forces generated by the data value equals 0. Calculation of inner cluster deviation (wc) for data of each chondrocyte variant, revealed that data points from all form three separate clusters, with the Control and MSC CM one, being only slightly separated, thus proving high similarity between mRNA expression of all analyzed genes in these two data groups.

Cellular localization of proteins encoded by SRI, SMC2, PSIP1, TLE4, and MSX1 genes

To validate the cellular localization of proteins encoded by *SRI*, *SMC2*, *PSIP1*, *TLE4*, and *MSX1* genes, we used the immunohistochemistry images of and immunofluorescence bone marrow and cartilage (chondrocytes from soft tissue) tissue sections stained with respective antibodies (method section), obtained from The Human Protein Atlas (Fig. 5.)[25]. Protein detection and staining intensity are presented in Table 4. Unfortunately, in the case of cartilage (chondrocytes), only Sorcin data were available (presenting strong staining intensity). Additionally, as data for Transducin-like enhancer of split protein 4 are not available for both bone marrow and cartilage, to further analyze cellular localization of all proteins, high-resolution immunofluorescence (confocal microscopy) images of U-2 OS human osteosarcoma cell line staining was presented. Even though U-2OS is not a cellular model of OA, it is often used to verify the subcellular localization of various proteins[26,27]. Structural Maintenance Of Chromosomes 2, PC4 and SRSF1 Interacting Protein 1, Transducin-like enhancer of split protein 4, and

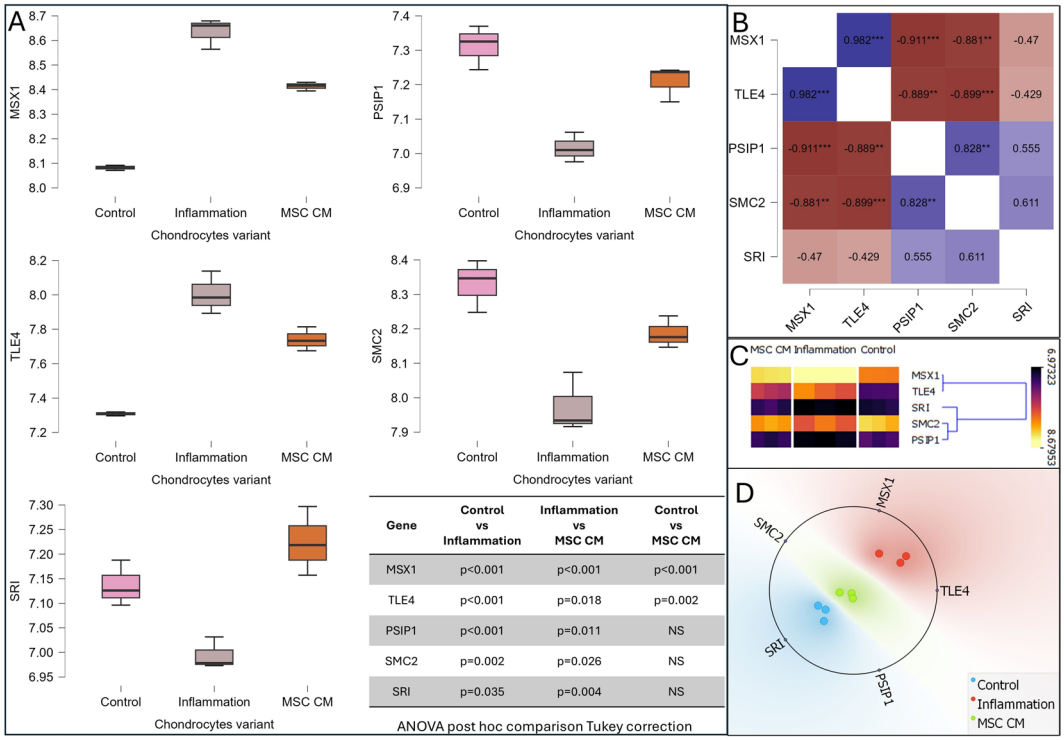

Gene	Control vs Inflammation	Inflammation vs MSC CM	Control vs MSC CM
MSX1	p<0.001	p<0.001	p<0.001
TLE4	p<0.001	p=0.018	p=0.002
PSIP1	p<0.001	p=0.011	NS
SMC2	p=0.002	p=0.026	NS
SRI	p=0.035	p=0.004	NS

Fig. 4. Analysis of selected genes as potential OA markers. The expression levels of selected *SRI*, *SMC2*, *PSIP1*, *TLE4*, and *MSX1* genes were analyzed using the GSE239343 dataset in the Control (chondrocytes), Inflammation (chondrocytes cultured in a mix of serum-free DMEM and 1% penicillin/streptomycin with 25 ng/mL TNF), MSC CM (chondrocytes cultured in a mix of serum-free DMEM and 1% penicillin/streptomycin with 25 ng/mL TNF and treated with 50 µg/mL of conditioned medium from adipose tissue-derived mesenchymal stem cells). Data were calculated using ANOVA with Tukey post hoc correction and visualized using JASP software (**A**). The Pearson correlation matrix was calculated and visualized using JASP software. The color intensity and presented value represent correlation efficiency whereas $*p<0.05$, $**p<0.005$, and $***p<0.001$ denote the statistical significance of the correlation (**B**). Hierarchical clustering analysis and hierarchical dendrogram were calculated and visualized using Orange data mining software (**C**). 2D depiction of mRNA expression level ability of data discrimination using Radial data visualization algorithm RadViz and *SRI*, *SMC2*, *PSIP1*, *TLE4*, and *MSX1* genes mRNA expression as attributes, calculated and visualized using Orange data mining software (**D**).

anti-Msh Homeobox 1 presents predominantly nucleoplasm localization, whereas Sorcin is present in both nucleoplasm and cytoplasm (Fig. 5.).

Molecular functions and biological pathways enrichment of proteins encoded by selected genes

To further elucidate the molecular functions of proteins encoded by *SRI*, *SMC2*, *PSIP1*, *TLE4*, and *MSX1* PPI network was composed using STRING version 12.0 online software (https://string-db.org/). Genes that were down-regulated and up-regulated in OA, were analyzed separately, using a minimal number of additional known proteins to fill missing connections and interactions (Fig. 6). The network created by *SRI*, *SMC2*, and *PSIP* separates into two distinct clusters with *SMC2*, and *PSIP* involved in the regulation of DNA condensation (GO:0000796 Condensin complex) and *SRI* in the regulation of lead ion binding and SOUL hem-binding protein (Fig. 6A). PPI network created using proteins encoded by *TLE4*, and *MSX1* proved involvement in the repression of Wingless and Int-1 (Wnt) target genes (HSA-4641265) (Fig. 6B). Finally, using the Pathway-to-Gene mode of the Pathway Connector tool we have analyzed additional biological pathways enriched and regulated by proteins encoded by selected genes (Fig. 6C). *PSIP1* enriches processes involved in the virus (including HIV) infection such as 2-LTR circle junctions of Viral DNA and integration of provirus. *SMC2* is involved in the condensation of chromatin and *SRI* in the transport of Ca2 + ions. The major pathway regulated by TLE4 is related to the repression of Wnt target genes. Unfortunately, the analyzed system version lacks *MSX1* interaction with known biological pathways.

Verification of chosen genes' feasibility as blood-derived OA markers

SRI, *SMC2*, *PSIP1*, *TLE4*, and *MSX1* were proven to be capable molecular markers (in cartilage and synovium) of knee OA and potential markers of OA regeneration upon MSCs treatment, that could be easily isolated in vitro. However, in vivo, knee biopsy is required, which might bring additional complications for patients. OA progression

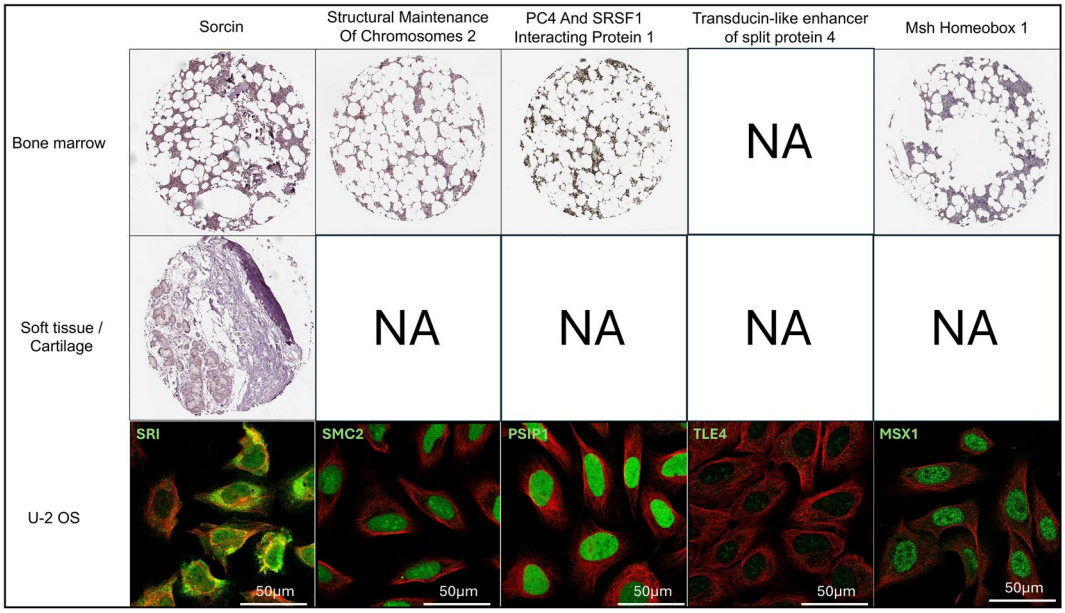

Fig. 5. Immunochemistry and immunofluorescence staining of proteins encoded by *SRI*, *SMC2*, *PSIP1*, *TLE4*, and *MSX1* genes. Data were obtained from the Human Protein Atlas database (https://www.proteinatlas.org/). NA – data not available. Detection and staining intensity are resented in Table 4. In the immunofluorescence staining, proteins encoded by *SRI*, *SMC2*, *PSIP1*, *TLE4*, and *MSX1* genes were shown as green, and microtubules as red. https://www.proteinatlas.org/ENSG00000075142-SRI/tissue/soft+tissue#imghttps://www.proteinatlas.org/ENSG00000075142-SRI/tissue/bone+marrow#imghttps://www.proteinatlas.org/ENSG00000136824-SMC2/tissue/bone+marrow#imghttps://www.proteinatlas.org/ENSG00000164985-PSIP1/tissue/bone+marrow#imghttps://www.proteinatlas.org/ENSG00000163132-MSX1/tissue/bone+marrow#imghttps://www.proteinatlas.org/ENSG00000136824-SMC2/subcellular#imghttps://www.proteinatlas.org/ENSG00000163132-MSX1/subcellular#imghttps://www.proteinatlas.org/ENSG00000075142-SRI/subcellular#imghttps://www.proteinatlas.org/ENSG00000106829-TLE4/subcellular#imghttps://www.proteinatlas.org/ENSG00000164985-PSIP1/subcellular#img.

Gene	Protein	Bone marrow	Cartilage
MSX1	Msh Homeobox 1	Not detected / Negative	NA
TLE4	Transducin-like enhancer of split protein 4	NA	NA
PSIP1	PC4 And SRSF1 Interacting Protein 1	High/strong	NA
SMC2	Structural Maintenance Of Chromosomes 2	Medium/moderate	NA
SRI	Sorcin	Low/moderate	High/strong

Table 4. Protein detection and staining intensity in bone marrow and cartilage. Data obtained from the HPA. NA- data not available.

triggers acute inflammation of the joint and its surrounding tissues leading to an acute systemic inflammatory response with increased cytokine and peripheral blood immune cell levels[28]. This prolonged inflammation may impact actual PBMC gene expression patterns, and several PBMC OA markers were previously identified[21,29]. Thus, we analyzed the potential role of our chosen genes as OA markers that could be potentially detected from the patient's blood[29]. The GSE48556 dataset, composed of transcriptomic data obtained from peripheral blood mononuclear cells of 33 healthy controls and 106 OA patients was downloaded[21]. Analysis of mRNA expression levels of chosen genes showed that only *PSIP1* and *TLE4* present statistically significant differences ($p < 0.001$) between PBMCs isolated from OA patients and healthy control (Fig. 7A). ROC analysis showed that AUC values of *PSIP1* and *TLE4* present lower values than 0.75, respectively 0.692 and 0.742, whereas, calculated precision equals 0.774 and 0.814 respectively (Fig. 7B). However, knowing that *PSIP1* mRNA expression is lower in PBMCs isolated from OA patients and *TLE4* is higher, we reasoned that *PSIP1:TLE4* mRNA expression ratio could be far more effective as a prognostic biomarker. Obtained values showed significant discriminating abilities of OA/control, with ROC analysis proving that the AUC value of *PSIP1:TLE4* equals 0.786 and a precision of 0.823 (Fig. 7C). Additionally due to sample size imbalance, sensitivity analysis was performed, down-sampling of the OA group, randomly assigning $n = 33$ OA samples using "data sampler" widget of orange data mining software. This analysis proved consistent results, supporting the robustness of our conclusions (data not shown).

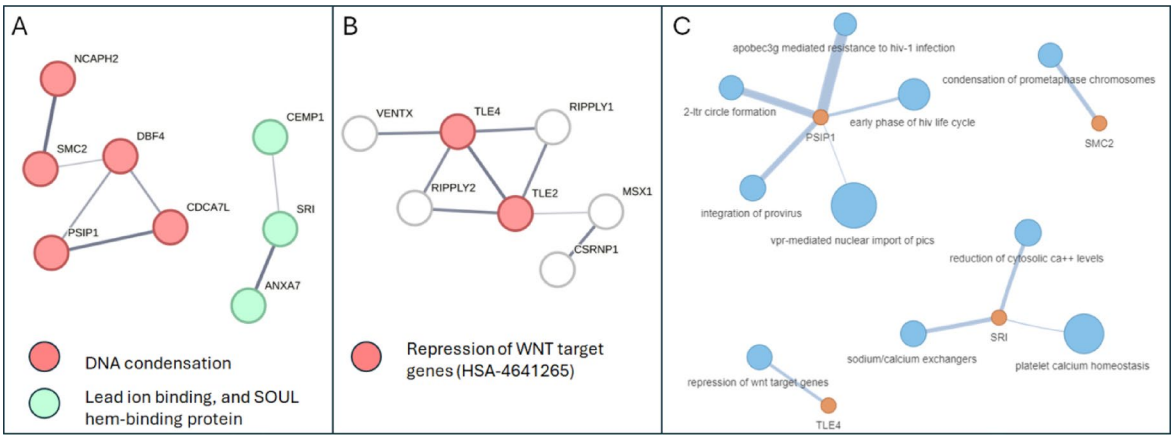

Fig. 6. Analysis of protein-protein interaction of *SRI*, *SMC2*, *PSIP1*, *TLE4*, and *MSX1* genes. PPI network of downregulated (**A**) and upregulated (**B**) genes in OA. Data visualized using the STRING platform. (**C**) Biological pathways enriched and regulated by proteins encoded by *PSIP1*, *SMC2*, *SRI*, and *TLE4* genes. Data analyzed and visualized using pathway-to-Gene analysis of the Pathway Connector tool and Reactome 2015 database.

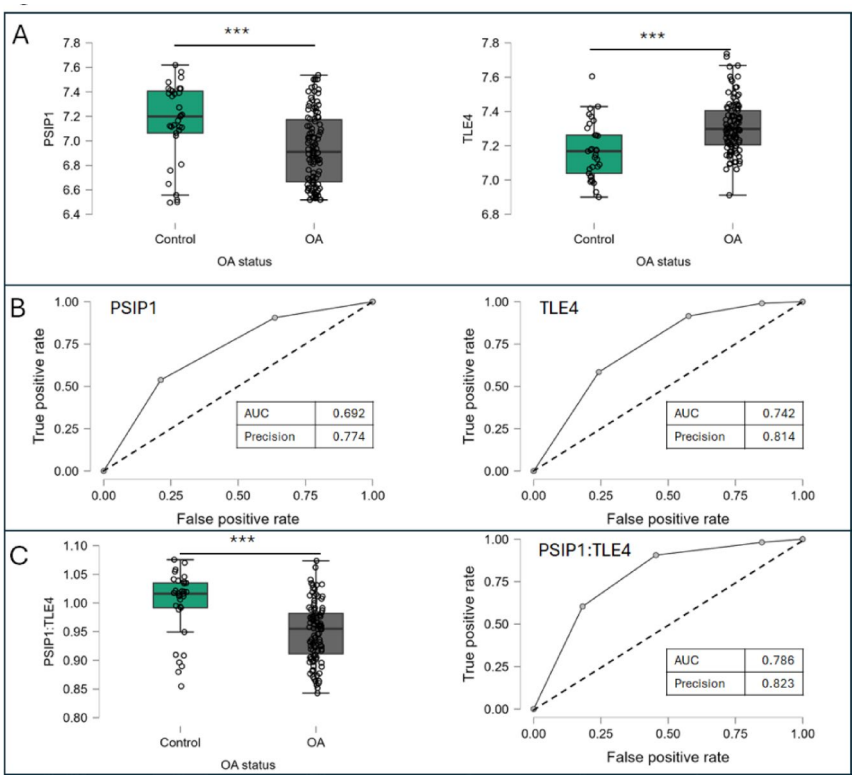

Fig. 7. Analysis of *PSIP1* and *TLE4* mRNA expression level in PBMCs as potential prognostic markers of OA development. mRNA expression levels of PSIP1 and TLE4 in PBMCs isolated from healthy (Control) and OA-affected (OA) patients (**A**). ROC analysis of prognostic properties of PBMCs mRNA levels of PSIP1 and TLE4 in OA development (**B**). Analysis of PBMCs isolated *PSIP1:TLE4* mRNA expression levels ratio as a prognostic tool of OA C). All calculations and visualizations were performed using Jasp software. Samples were tested with the Shapiro–Wilk test, presenting a not-normal distribution, thus followed by the Mann-Whitney U test *** $p < 0.001$.

Discussion

Annually, millions of patients around the world, suffer from OA-related mild to severe joint pain and movement impediments leading to long-term disabilities. OA's economic and social impact can not be dismissed, especially considering the aging society and increasing obesity rate[1,2,5]. Thus, since currently, no drugs can alter the

progression of OA, the development of new therapeutic strategies such as regenerative therapy is extremely important. The first concept of regenerative therapy in OA assumed that administered cells may engraft to a lesion site and differentiate into chondrocytes with autologous chondrocytes being the first cell candidates[30]. Unfortunately, important shortcomings of such treatment modality, including loss of chondrocyte phenotypes and additional problems associated with the process of chondrocyte acquisition, led scientists to search for other sources of therapeutic cells, predominantly mesenchymal stem cells (derived from either: bone marrow, umbilical cord, or adipose tissue)[12,30]. However, we lack well-established molecular indicators of OA advancement. Currently, serious efforts are focused on the molecular understanding of the disease, that could be utilized to address disease prevention, diagnosis, and treatment leading to the qualification of biomarkers, intended for use as companion diagnostics for approval of a new drug or therapeutic scheme[31]. Therefore, we have focused on establishing potential molecular markers, that, on the mRNA level, would allow us to monitor OA development, progression, and potential MSC-based regeneration of OA-affected cells (in vitro) and tissue (in vivo).

In our study, we have focused on the knee joint as one of the most prevalent sites[3]. Our analysis proved that aurora B and A signaling pathways are significantly enriched in OA-affected chondrocytes but not in synovium. Aurora kinase B (AURKB) is a key component of the chromosomal passenger complex involved in heterochromatin destabilization and mitosis progression, which in the case of OA-affected chondrocytes may induce senescence, leading to MMPs overexpression and OA progression[32]. Nevertheless, both OA-affected knee synovium and knee chondrocytes present similar enrichment of major biological pathways that are dysregulated during OA progression (such as PDGF, IGF1, VEGF, S1P1, glypican or TRAIL signaling pathways). Thus, in the first step, we have identified dysregulated genes for both (patient-derived) synovium and chondrocytes, focusing on those presented in both OA-affected cell types. This approach allowed us to select up and down-regulated genes that are generally relevant to OA development. Enrichment analysis proved that selected up- and down-regulated genes are involved mainly in the process such as apoptosis, immune response, cell proliferation, cell adhesion, migration, cell-matrix degradation, and ion transport. Apoptosis as an etiological factor in osteoarthritis onset, combined with dysregulated immune response and impaired cell-matrix interactions, often leads to increased and prolonged inflammation and cartilage or tendon tissue degradation, contributing to the significant deterioration of the patient's condition[4,21]. PPI networks created by up and down-regulated genes that are generally relevant to OA development present a similar value of average ClusteringCoefficient parameter, which is a numerical depiction of how interconnected a node's neighbors are, enabling quantification of the local cohesiveness of interactions. Low average BetweennessCentrality and high average Degree parameter in both networks suggests that the majority of the nodes are less involved in connecting distant parts of the network, and few proteins, such as AKT1 (Degree 22) and EGFR (Degree 44), act as key bottleneck hubs, regulating signaling pathways related to the development of OA[6,33,34]. Additionally, higher average ClosenessCentrality in the PPI network of up-regulated genes suggests higher signaling efficiency of hub genes.

Next, we have shifted our interest to an in vitro model of OA caused by TNF-derived inflammation of chondrocytes to identify potential new markers of OA reversion via the regenerative properties of AD-MSCs secretome[20]. TNF-treated chondrocytes, presents molecular characteristic of in vivo OA affected cartilage, especially regarding expression of well know OA markers such as: *IL-1B*, *IL6*, *MMP1*, *MMP2*, *MMP3*, *MMP9*, *MMP13* and *ADAMTS5*. Analyzed data were verified using previously obtained DEGs (patient-derived) that are generally relevant to OA development. Selected genes *SRI*, *SMC2*, *PSIP1*, *TLE4*, and *MSX1* presented dysregulated expression levels in the TNF-inflammation-derived in vitro model of OA, as well as in patient samples – compared to respective non-OA controls, and their expression levels were reversed to control level upon AD-MSCs secretome treatment.

All proteins encoded by chosen genes present nucleoplasm localization, with only Sorcin (soluble resistance-related calcium-binding protein) encoded by SRI being detected in both nucleoplasm and cytoplasm (predominantly). Cell nuclei, with well-defined chromatin compartmentalization and ribosome biogenesis, is a key player that regulates many aspects of cell biology. Therefore, nucleoplasm proteins are extremely sensitive even to incremental changes in cell physiology, which can be exploited to monitor cores of the disease[35]. Sorcin is a key protein in the endoplasmic reticulum (ER) calcium-dependent cascades and signaling that regulates cellular homeostasis via important functions, such as gene expression, cell differentiation, proliferation, survival, apoptosis, and xenobiotics (drugs) resistance[36,37]. Interestingly, Gong et al. observed different levels of extracellular calcium-dependent spontaneous signaling between different zones in healthy cartilage, whereas this zonal difference was not observed in OA-affected cartilage, proving that an imbalance in calcium signaling relates to OA[38]. The protein encoded by *SMC2* is involved in the regulation of chromosome condensation during mitosis[39]. There are no known alterations regarding SMC2 and OA development, however, it is a known fact that SMC2 downregulation and/or knock-out impairs bovine embryo development[40]. Interestingly, SMC2 was proven to be one of the top hub genes involved in dynamic compression-enhanced chondrogenesis leading to cartilage regeneration[8]. PC4 And SRSF1 Interacting Protein 1 also known as Lens epithelium-derived growth factor is a transcriptional co-activator and cellular stress survival factor regulating processes such as DNA repair and RNA transcription essential for the cell/tissue development. PSIP1 plays an important role in the course of several human diseases, including acute leukemia, virus infection, and autoimmune disorders[41]. Proteins encoded by *SMC2* and *PSIP1* genes, via regulation of chromatin condensation, influence the expression of many, potentially OA-related genes. Transducin-like enhancers of split protein 4 (TLE4), share identical structures and molecular properties as the Drosophila protein Groucho which is involved in the regulation of cell-determination events during insect neurogenesis and segmentation. Its expression pattern correlates to TLE2[42]. TLE4 and TLE2 transcriptionally repress Wnt-β-catenin signaling, repressing Wnt-mediated inflammation[43]. In the case of OA, a positive correlation between disease severity and Wnt-β-catenin signaling was observed, thus upregulation of its repressor in the OA-affected cells, at first sight, is rather surprising and difficult to explain[44]. However, canonical (Wnt/β-catenin, Wnt3a) and non-canonical (β-catenin independent, Wnt5a) Wnt signaling

pathways substantially differ, influencing transcription of target genes via (respectively) β-catenin or Jun/ATF2 and NAFT transcription factors[45]. Furthermore, there is substantial heterogeneity within OA patients and caused by the multifactorial nature of this disease. Canonical Wnt signaling plays a major role in injury-induced osteoarthritis mouse models but is not observed in the STR/ort mouse OA model[46]. Treatment of OA-affected sheep cartlidge with Wnt signaling antagonist - sclerostin, results in inhibition of Wnt/β-catenin signaling and predominately an anti-catabolic effect by reducing *Mmp*, *Adamts*, *Acan*, and *Col2a1* gene expression, as well as IL-1*a*-mediated aggrecanolysis[47]. The complex nature of the Wnt regulatory network in skeletal homeostasis proves that both excessive activation and inactivation of Wnt signaling can cause skeletal malformation, bone diseases, and cartilage loss. Recent reports suggest that Wnt16 presents a strong association with bone mineral density and strength, overall cortical bone thickness, additionally playing a chondroprotective role, limiting cartilage destruction during OA progression[48]. Associated with bone formation, the *MSX1* gene was previously shown by Karlsson et al. to be significantly upregulated in OA-affected cartilage compared to normal (ON-not-affected) control cartilage[49]. On the other hand, recent studies have shown that *MSX1*$^{+}$ mesenchymal progenitor cells exhibit strong chondrogenic potential, that could be utilized for cartilage regeneration. In the rat models of acute rotator cuff injury, overexpression of the *Msx1* inhibits osteogenic and chondrogenic differentiation of the engrafted bone marrow mesenchymal stem cells simultaneously increasing their differentiation and migratory potential[50]. Thus, the role of MSX1 in OA development and cartilage damage and regeneration requires further analysis.

Accurate molecular markers for monitoring OA progression and regeneration, which are valid in patients, are essential for in vitro studies to develop new therapies. However, in the case of OA patients, analysis of their expression (thus monitoring of OA regeneration) would require constant joint biopsy. Therefore, less invasive methods, of OA marker isolation, such as blood liquid biopsy are being developed[29,51]. Progression of OA is related to the inflammation and recruitment of immunological cells which can impact actual PBMC gene expression, leading to the identification of PBMC-derived OA markers[21,29,52]. Interestingly, our data proves the expression level of *PSIP1* and *TLE4* in the PMBCs correlates with OA development, however, when used separately, as a single prognostic marker, each of them presents less than 0.75 ROC AUC, thus poor discrimination. On the other hand, the *PSIP1:TLE4* mRNA expression levels ratio used as a prognostic marker presents AUC for ROC 0.786, which could be regarded as more than acceptable.

The major limitation of this study is that data, are obtained mainly from the European descent population of Western society (mainly due to the higher OA incident rate). Consequently, our findings may not account for racial-specific factors, especially in the light of the evidence that in the case of knee OA, pain and functional limitations are greater for African and African-Americans than European descent[4,53]. Additionally, we have based our analysis on available clinical descriptions of patients' OA status. However, standard MRI are focused mostly on alterations seen in advanced OA stages possibly incorrectly identifying early, potentially reversible stages[14]. Furthermore, GSE48556 dataset consists of imbalanced sample size (33 healthy subjects and 106 OA patients) and highlights one of the biggest problems with clinical data, that disease cohorts are usually better characterized than healthy controls. Additionally, we have based our study on microarray data that are less sensitive than RNA sequencing (RNA-seq) especially for low-abundance RNAs (Spearman correlations coefficients of ~0.8 between expression data obtained from the Affymetrix one-channel microarray and RNAseq for high-abundance genes and ~0.2 for low-abundance genes), but are more reliable and easier to use regarding analysis of gene expression profiling of well-know sequences. Furthermore, results derived from microarrays accumulated over the last 20 years, and stored in repositories such as GEO, can still serve as excellent data mining resources[54,55]. Finally, despite the fact that recent transcriptomic analyses of OA patient samples deposited in the GEO database, have indeed yielded clinically valuable insights, particularly for potential new biomarker discovery and therapeutic targets, translating these findings into real-world clinical practice requires additional experimental confirmation and preferably prospective or controlled clinical studies[56,57].

Conclusion

Our analysis proved that mRNA expression levels of *SRI*, *SMC2*, *PSIP1*, *TLE4*, and *MSX1* are dysregulated in osteoarthritis (*SRI*, *SMC2*, *PSIP1* downregulated in OA, *TLE4*, and *MSX1* upregulated in OA) and potentially could be utilized to monitor its development and potential regeneration upon AD-MSCs-based regenerative therapy in both chondrocytes and synovium. Additionally, expression levels of *PSIP1* and *TLE4* in the PMBCs may be considered as less invasive OA markers. These genes have potential as diagnostic and prognostic biomarkers not only in osteoarthritis but also in other chronic joint diseases, traumatic injuries, and overuse syndromes. Further research is needed to validate their clinical utility across these diverse conditions.

Data availability

The datasets analyzed during the current study are available in the Gene Expression Omnibus repository at http://www.ncbi.nlm.nih.gov/geo/ reference numbers: GSE239343, GSE179716, GSE206848 and GSE48556. URLs: https://www.ncbi.nlm.nih.gov/geo/query/acc.cgi?acc=GSE239343, https://www.ncbi.nlm.nih.gov/geo/query/acc.cgi?acc=GSE179716, https://www.ncbi.nlm.nih.gov/geo/query/acc.cgi?acc=GSE206848, https://www.ncbi.nlm.nih.gov/geo/query/acc.cgi?acc=GSE48556.

Received: 11 April 2025; Accepted: 24 July 2025
Published online: 20 August 2025

References

1. Leifer, V. P., Katz, J. N. & Losina, E. Chap. 1: the burden of OA-health services and economics. *Osteoarthr. Cartil.* **30**, 10–16. https://doi.org/10.1016/j.joca.2021.05.007 (2022).
2. Long, H. et al. Prevalence Trends of Site-Specific Osteoarthritis From 1990 to 2019: Findings From the Global Burden of Disease Study 2019, *Arthritis Rheumatol.* **74** 1172–1183. https://doi.org/10.1002/art.42089. (2022).
3. Boer, C. G. et al. Deciphering osteoarthritis genetics across 826,690 individuals from 9 populations. *Cell.* **184**, 4784–4818.e17. https://doi.org/10.1016/j.cell.2021.07.038 (2021).
4. Yao, Q. et al. Osteoarthritis: pathogenic signaling pathways and therapeutic targets. *Sig Transduct. Target. Ther.* **8**, 1–31. https://doi.org/10.1038/s41392-023-01330-w (2023).
5. Xiang, Q. et al. Cellular and molecular mechanisms underlying obesity in degenerative spine and joint diseases. *Bone Res.* **12**, 71. https://doi.org/10.1038/s41413-024-00388-8 (2024).
6. Li, H. et al. TNF-α increases the expression of inflammatory factors in synovial fibroblasts by inhibiting the PI3K/AKT pathway in a rat model of monosodium iodoacetate-induced osteoarthritis. *Exp. Ther. Med.* **16**, 4737–4744. https://doi.org/10.3892/etm.2018.6770 (2018).
7. Chisari, E., Yaghmour, K. M. & Khan, W. S. The effects of TNF-alpha inhibition on cartilage: a systematic review of preclinical studies. *Osteoarthr. Cartil.* **28**, 708–718. https://doi.org/10.1016/j.joca.2019.09.008 (2020).
8. Chen, J., Chen, L., Hua, J. & Song, W. Long-term dynamic compression enhancement TGF-β3-induced chondrogenesis in bovine stem cells: a gene expression analysis. *BMC Genom Data*. **22**, 13. https://doi.org/10.1186/s12863-021-00967-2 (2021).
9. Lohmander, L. S. & Roos, E. M. Disease modification in OA — will we ever get there? *Nat. Rev. Rheumatol.* **15**, 133–135. https://doi.org/10.1038/s41584-019-0174-1 (2019).
10. Richard, M. J., Driban, J. B. & McAlindon, T. E. Pharmaceutical treatment of osteoarthritis. *Osteoarthr. Cartil.* **31**, 458–466. https://doi.org/10.1016/j.joca.2022.11.005 (2023).
11. Zhang, W., Robertson, W. B., Zhao, J., Chen, W. & Xu, J. Emerging trend in the pharmacotherapy of osteoarthritis. *Front. Endocrinol.* **10** https://doi.org/10.3389/fendo.2019.00431 (2019).
12. Zhu, C., Wu, W. & Qu, X. Mesenchymal stem cells in osteoarthritis therapy: a review. *Am. J. Transl Res.* **13**, 448–461 (2021).
13. Tortorella, F. et al. Meniscal extrusion correlates with symptom severity in knee osteoarthritis: an ultrasound and magnetic resonance imaging analysis of 100 patients. *J. Clin. Med.* **13**, 7716. https://doi.org/10.3390/jcm13247716 (2024).
14. Mallio, C. A. et al. Advanced MR imaging for knee osteoarthritis: A review on local and brain effects. *Diagnostics (Basel)*. **13**, 54. https://doi.org/10.3390/diagnostics13010054 (2022).
15. Wei, Q. et al. Plasma proteomics implicate glutamic oxaloacetic transaminases as potential markers for acute myocardial infarction. *J. Proteom.* **308**, 105286. https://doi.org/10.1016/j.jprot.2024.105286 (2024).
16. Kryczka, J. & Boncela, J. Integrated bioinformatics analysis of the hub genes involved in Irinotecan resistance in colorectal cancer. *Biomedicines* **10**, 1720. https://doi.org/10.3390/biomedicines10071720 (2022).
17. Kryczka, J., Bachorz, R. A., Kryczka, J. & Boncela, J. Radial data visualization-based step-by-step eliminative algorithm to predict colorectal cancer patients' response to FOLFOX therapy. *Int. J. Mol. Sci.* **25**, 12149. https://doi.org/10.3390/ijms252212149 (2024).
18. Tahir, M. et al. Artificial intelligence and deep learning algorithms for epigenetic sequence analysis: A review for epigeneticists and AI experts. *Comput. Biol. Med.* **183**, 109302. https://doi.org/10.1016/j.compbiomed.2024.109302 (2024).
19. Jafari, M. & Ansari-Pour, N. Why, when and how to adjust your P values?? *Cell. J.* **20**, 604–607. https://doi.org/10.22074/cellj.2019.5992 (2019).
20. González-Cubero, E. et al. The therapeutic potential of adipose-derived mesenchymal stem cell secretome in osteoarthritis: A comprehensive study. *Int. J. Mol. Sci.* **25**, 11287. https://doi.org/10.3390/ijms252011287 (2024).
21. Ramos, Y. F. M. et al. Genes expressed in blood link osteoarthritis with apoptotic pathways. *Ann. Rheum. Dis.* **73**, 1844–1853. https://doi.org/10.1136/annrheumdis-2013-203405 (2014).
22. Koren, Y. & Carmel, L. Visualization of labeled data using linear transformations. In *IEEE Symposium on Information Visualization 2003* (IEEE Cat. No.03TH8714), 121–128. https://doi.org/10.1109/INFVIS.2003.1249017 (2003).
23. Leban, G., Zupan, B., Vidmar, G. & Bratko, I. VizRank: Data Visualization Guided by Machine Learning, *Data Min. Knowl. Disc* **13** 119–136. https://doi.org/10.1007/s10618-005-0031-5. (2006).
24. Kryczka, J. & Boncela, J. Characteristics of ABCC4 and ABCG2 high expression subpopulations in CRC-A new opportunity to predict therapy response. *Cancers (Basel)*. **15**, 5623. https://doi.org/10.3390/cancers15235623 (2023).
25. Uhlén, M. et al. A human protein atlas for normal and cancer tissues based on antibody proteomics. *Mol. Cell. Proteom.* **4**, 1920–1932. https://doi.org/10.1074/mcp.M500279-MCP200 (2005).
26. Beijer, D. et al. Biallelic ADPRHL2 mutations in complex neuropathy affect ADP ribosylation and DNA damage response. *Life Sci. Alliance*. **4** https://doi.org/10.26508/lsa.202101057 (2021).
27. Nusinow, D. P. et al. Quantitative proteomics of the cancer cell line encyclopedia. *Cell.* **180** 387–402.e16. https://doi.org/10.1016/j.cell.2019.12.023. (2020).
28. Weber, P. et al. Zenobi-Wong, the collagenase-induced osteoarthritis (CIOA) model: where mechanical damage meets inflammation. *Osteoarthr. Cartil. Open.* **6**, 100539. https://doi.org/10.1016/j.ocarto.2024.100539 (2024).
29. Li, Y. & Dong, B. Exploring liquid-liquid phase separation-related diagnostic biomarkers in osteoarthritis based on machine learning algorithms and experiment. *Immunobiology* **229**, 152825. https://doi.org/10.1016/j.imbio.2024.152825 (2024).
30. Im, G. I. & Kim, T. K. Regenerative therapy for osteoarthritis: A perspective. *Int. J. Stem Cells.* **13**, 177–181. https://doi.org/10.15283/ijsc20069 (2020).
31. Kraus, V. B. Biomarkers as drug development tools: discovery, validation, qualification and use. *Nat. Rev. Rheumatol.* **14**, 354–362. https://doi.org/10.1038/s41584-018-0005-9 (2018).
32. Ren, X., Zhuang, H., Jiang, F., Zhang, Y. & Zhou, P. Barasertib impedes chondrocyte senescence and alleviates osteoarthritis by mitigating the destabilization of heterochromatin induced by AURKB. *Biomed. Pharmacother.* **166**, 115343. https://doi.org/10.1016/j.biopha.2023.115343 (2023).
33. Xie, J. et al. Sustained Akt signaling in articular chondrocytes causes osteoarthritis via oxidative stress-induced senescence in mice. *Bone Res.* **7**, 23. https://doi.org/10.1038/s41413-019-0062-y (2019).
34. Wei, Y. et al. Targeting cartilage EGFR pathway for osteoarthritis treatment. *Sci. Transl. Med.* **13**, eabb3946. https://doi.org/10.1126/scitranslmed.abb3946 (2021).
35. Su, H., Kodiha, M., Lee, S. & Stochaj, U. Identification of novel markers that demarcate the nucleolus during severe stress and chemotherapeutic treatment. *PLoS One*. **8**, e80237. https://doi.org/10.1371/journal.pone.0080237 (2013).
36. Ghosh, S., Sharma, A., Kumar, R. S. & Nasare, V. Sorcin: mechanisms of action in cancer hallmarks, drug resistance and opportunities in therapeutics. *Med. Oncol.* **42**, 29. https://doi.org/10.1007/s12032-024-02580-6 (2024).
37. Genovese, I. et al. Sorcin is an early marker of neurodegeneration, Ca2 + dysregulation and endoplasmic reticulum stress associated to neurodegenerative diseases. *Cell. Death Dis.* **11**, 861. https://doi.org/10.1038/s41419-020-03063-y (2020).
38. Gong, X. et al. Altered spontaneous calcium signaling of in situ chondrocytes in human osteoarthritic cartilage. *Sci. Rep.* **7**, 17093. https://doi.org/10.1038/s41598-017-17172-w (2017).
39. Song, W. M. et al. Multiscale protein networks systematically identify aberrant protein interactions and oncogenic regulators in seven cancer types. *J. Hematol. Oncol.* **16**, 120. https://doi.org/10.1186/s13045-023-01517-2 (2023).
40. Alba, P. G. et al. Pablo, SMC2 ablation impairs bovine embryo development shortly after blastocyst hatching. *Reproduction* **168**, e240211. https://doi.org/10.1530/REP-24-0211 (2024).

41. Brouns, T. et al. The impact of lens epithelium-derived growth factor p75 dimerization on its tethering function. *Cells* **13**, 227. https://doi.org/10.3390/cells13030227 (2024).
42. Yao, J. et al. Combinatorial expression patterns of individual TLE proteins during cell determination and differentiation suggest non-redundant functions for mammalian homologs of drosophila Groucho. *Dev. Growth Differ.* **40**, 133–146. https://doi.org/10.1046/j.1440-169x.1998.00003.x (1998).
43. Shin, T. H., Brynczka, C., Dayyani, F., Rivera, M. N. & Sweetser, D. A. TLE4 regulation of wnt-mediated inflammation underlies its role as a tumor suppressor in myeloid leukemia. *Leuk. Res.* **48**, 46–56. https://doi.org/10.1016/j.leukres.2016.07.002 (2016).
44. Zheng, H. et al. An injectable hydrogel loaded with Icariin attenuates cartilage damage in rabbit knee osteoarthritis via Wnt/β-catenin signaling pathway. *Int. Immunopharmacol.* **145**, 113725. https://doi.org/10.1016/j.intimp.2024.113725 (2025).
45. Shi, D. L. Canonical and non-canonical Wnt signaling generates molecular and cellular asymmetries to establish embryonic axes. *J. Dev. Biology*. **12**, 20. https://doi.org/10.3390/jdb12030020 (2024).
46. Poulsen, R. C., Jain, L. & Dalbeth, N. Re-thinking osteoarthritis pathogenesis: what can we learn (and what do we need to unlearn) from mouse models about the mechanisms involved in disease development. *Arthritis Res. Therapy*. **25**, 59. https://doi.org/10.1186/s13075-023-03042-6 (2023).
47. Zhou, Y., Wang, T., Hamilton, J. L. & Chen, D. Wnt/β-catenin signaling in osteoarthritis and in other forms of arthritis. *Curr. Rheumatol. Rep.* **19**, 53. https://doi.org/10.1007/s11926-017-0679-z (2017).
48. Ye, X. & Liu, X. Wnt16 signaling in bone homeostasis and osteoarthristis. *Front. Endocrinol. (Lausanne)*. **13**, 1095711. https://doi.org/10.3389/fendo.2022.1095711 (2022).
49. Karlsson, C. et al. Genome-wide expression profiling reveals new candidate genes associated with osteoarthritis. *Osteoarthr. Cartil.* **18**, 581–592. https://doi.org/10.1016/j.joca.2009.12.002 (2010).
50. Liu, K., Fu, X. W. & Wang, Z. M. Msx1-modified rat bone marrow mesenchymal stem cell therapy for rotator cuff repair: A comprehensive analysis of tendon-bone healing and cellular mechanisms. *J. Orthop. Res.* https://doi.org/10.1002/jor.26039 (2024).
51. Tchetina, E. et al. Upregulation measured in the peripheral blood mononuclear cells prior to surgery points to postoperative pain development in patients with hip osteoarthritis. *Diagnostics* **13**, 1739. https://doi.org/10.3390/diagnostics13101739 (2023).
52. Hu, S., Tao, Y., Hu, F. & Liu, X. Diminished LAG3 + B cells correlate with exacerbated rheumatoid arthritis. *Ann. Med.* **55**, 2208373. https://doi.org/10.1080/07853890.2023.2208373 (2023).
53. Allen, K. D. Racial and ethnic disparities in osteoarthritis phenotypes. *Curr. Opin. Rheumatol.* **22**, 528–532. https://doi.org/10.1097/BOR.0b013e32833b1b6f (2010).
54. Guo, Y. et al. Large Scale Comparison of Gene Expression Levels by Microarrays and RNAseq Using TCGA Data, *PLoS One* **8** e71462. https://doi.org/10.1371/journal.pone.0071462. (2013).
55. Mantione, K. J. et al. Comparing bioinformatic gene expression profiling methods: microarray and RNA-Seq. *Med. Sci. Monit. Basic. Res.* **20**, 138–141. https://doi.org/10.12659/MSMBR.892101 (2014).
56. He, M. et al. Screening and validation of key genes associated with osteoarthritis. *BMC Musculoskelet. Disord.* **25**, 954. https://doi.org/10.1186/s12891-024-08015-7 (2024).
57. Zhu, Y. S., Yan, H., Mo, T. T., Zhang, J. N. & Jiang, C. Identification of diagnostic markers in synovial tissue of osteoarthritis by weighted gene coexpression network. *Biochem. Genet.* **61**, 2056–2075. https://doi.org/10.1007/s10528-023-10359-z (2023).

Acknowledgements

The authors gratefully acknowledge the Polish Muscles Ligaments and Tendons Society (PolMuLTS) for the constructive feedback.The authors declare that they have not use AI-generated work in this manuscript.

Author contributions

J.K.: investigation, methodology, writing—original draft, formal analysis; validation.E.B-L.: formal analysis, writing—review and editing. M.P.: formal analysis; writing—review and editing. J.B.: funding acquisition; project administration; formal analysis; writing—review and editing. J.M.K.: conceptualization; data curation; formal analysis; investigation; methodology; project administration; resources; software; supervision; validation; visualization; writing—original draft.

Funding

This research was supported by the statutory fund of the Institute of Medical Biology of the Polish Academy of Sciences.

Declarations

Competing interests

The authors declare no competing interests.

Additional information

Correspondence and requests for materials should be addressed to J.M.K.